Journal Pre-proof

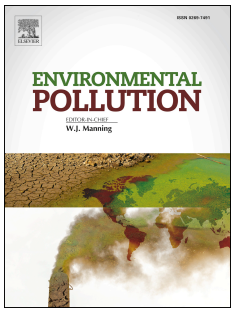

Forchlorfenuron (CPPU) causes disorganization of the cytoskeleton and dysfunction of human umbilical vein endothelial cells, and abnormal vascular development in zebrafish embryos

Guiyi Gong, Hiotong Kam, Yu-chung Tse, John P. Giesy, Sai-wang Seto, Simon Ming-yuen Lee

PII: S0269-7491(20)36480-0

DOI: https://doi.org/10.1016/j.envpol.2020.115791

Reference: ENPO 115791

To appear in: *Environmental Pollution*

Received Date: 6 July 2020

Revised Date: 23 September 2020

Accepted Date: 5 October 2020

Please cite this article as: Gong, G., Kam, H., Tse, Y.-c., Giesy, J.P., Seto, S.-w., Lee, S.M.-y., Forchlorfenuron (CPPU) causes disorganization of the cytoskeleton and dysfunction of human umbilical vein endothelial cells, and abnormal vascular development in zebrafish embryos, *Environmental Pollution*, https://doi.org/10.1016/j.envpol.2020.115791.

Guiyi Gong: Conceptualization; Formal analysis; Investigation; Methodology; Validation; Roles/Writing - original draft;
Hiotong Kam: Visualization; Software; Validation; Investigation;
Yuchung Tse: Data curation; Formal analysis; Methodology;
John P. Giesy: Writing - review & editing.
Sai-wang Seto: Review & editing
Simon Mingyuen Lee: Funding acquisition; Methodology; Project administration; Resources; Supervision; Writing - review & editing.

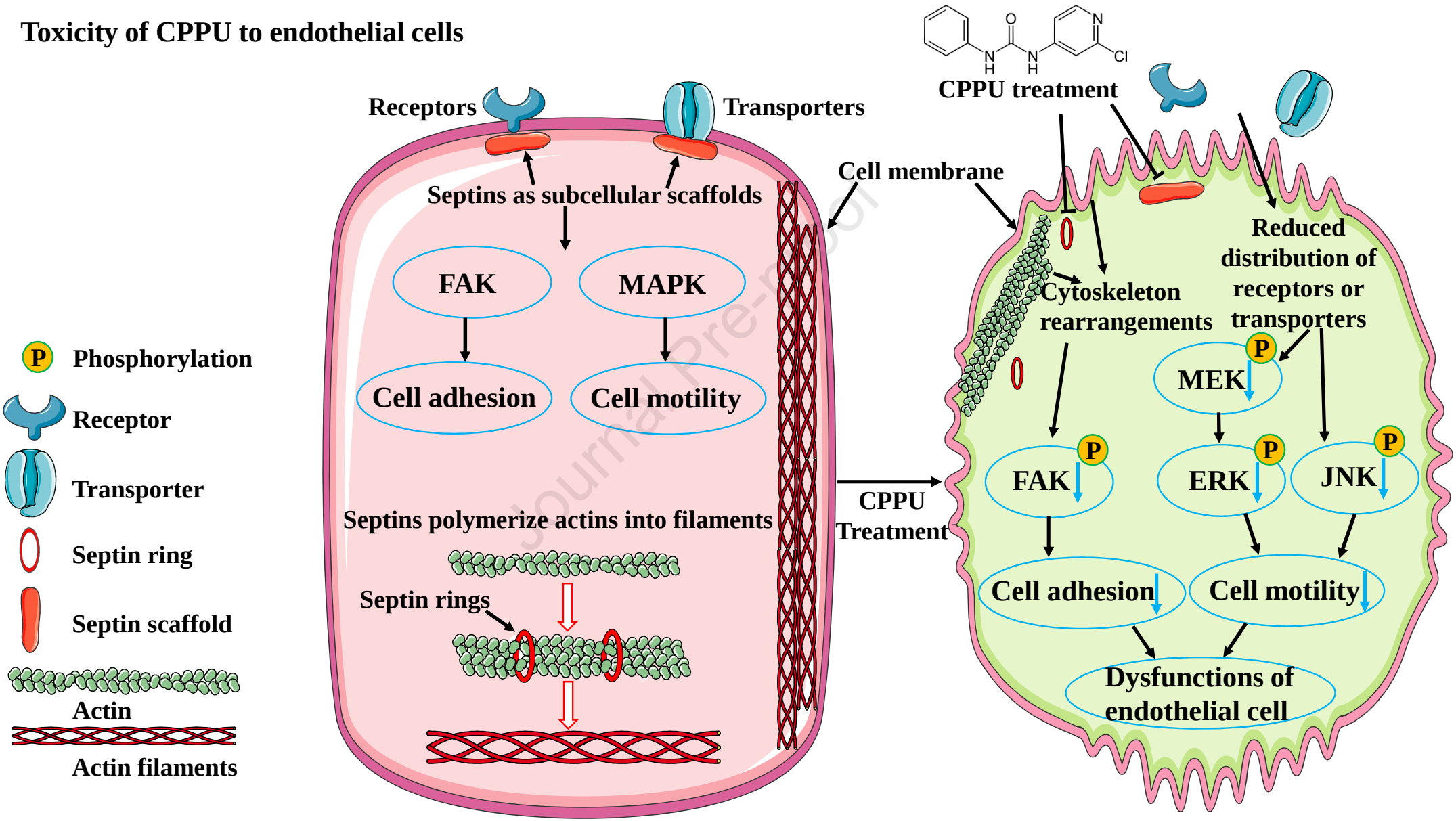

Forchlorfenuron (CPPU) causes disorganization of the cytoskeleton and dysfunction of human umbilical vein endothelial cells, and abnormal vascular development in zebrafish embryos

Guiyi Gong [a,b], Hiotong Kam [a], Yu-chung Tse [b], John P. Giesy [c,d,e], Sai-wang Seto [f], Simon Ming-yuen Lee [a,*]

[a] State Key Laboratory of Quality Research in Chinese Medicine and Institute of Chinese Medical Sciences, University of Macau, Macau, China.

[b] Guangdong Provincial Key Laboratory of Cell Microenvironment and Disease Research, Department of Biology, Southern University of Science and Technology (SUSTech), Shenzhen, 518055, China.

[c] Toxicology Centre, University of Saskatchewan, Saskatoon, Saskatchewan S7N 5B3, Canada

[d] Department of Veterinary Biomedical Sciences, University of Saskatchewan, Saskatoon, Saskatchewan S7N 5B4, Canada

[e] Department of Environmental Sciences, Baylor University, Waco, TX 76706, United States

[f] Department of Applied Biology and Chemistry Technology, The Hong Kong Polytechnic University, Hung Hom, Kowloon, Hong Kong, China

[*]Corresponding authors:

Simon Ming Yuen Lee, E-mail addresses: simonlee@umac.mo

Abstract

Forchlorfenuron (CPPU) has been used worldwide, to boost size and improve quality of various agricultural products. CPPU and its metabolites are persistent and have been detected frequently in fruits, water, sediments, and organisms in aquatic systems. Although the public became aware of CPPU through the exploding watermelon scandal of 2011 in Zhenjiang, China, little was known of its potential effects on the environment and wildlife. In this study, adverse effects of CPPU on developmental angiogenesis and vasculature, which is vulnerable to insults of persistent toxicants, were studied *in vivo* in zebrafish embryos (*Danio rerio*). Exposure to 10 mg CPPU/L impaired survival and hatching, while development was hindered by exposure to 2.5 mg CPPU/L. Developing vascular structure, including common cardinal veins (CCVs), intersegmental vessels (ISVs) and sub-intestinal vessels (SIVs), were significantly restrained by exposure to CPPU, in a dose-dependent manner. Also, CPPU caused disorganization of the cytoskeleton. In human umbilical vein endothelial cells (HUVECs) CPPU inhibited proliferation, migration and formation of tubular-like structures *in vitro*. Results of western blot analyses revealed that exposure to CPPU increased phosphorylation of FLT-1, but inhibited phosphorylation of FAK and its downstream MAPK pathway in HUVECs. In summary, CPPU elicited developmental toxicity to the developing endothelial system of zebrafish and HUVECs. This was do, at least in part due to inhibition of the FAK/MAPK signaling pathway rather than direct interaction with the VEGF receptor (VEGFR).

Main finding

Forchlorfenuron (CPPU) affected HUVECs *in vitro* and development of zebrafish embryos *in vivo*.

Keywords:
Toxicity; HUVECs, Blood vessels, Septin, crop growth promotor.

Introduction

Some agrochemicals can affect non-target organisms during use (Barmentlo et al., 2018; Rundlof and Lundin, 2019). Subsequently, repetitive use of agrochemicals can decrease biodiversity, while continuous and non-judicious use of agrochemicals can contaminate food and the environment, which are associated with exposures to and potential effects on wildlife and humans (Carvalho, 2017; Gyenwali et al., 2017; Solomon et al., 2000). In humans, exposure to pesticides has been associated with various cardiovascular diseases, such as atherosclerosis (Curl et al., 2015), cerebrovascular diseases (CVDs), myocardial infarction, and stroke (Kim et al., 2015; Lind and Lind, 2012; Sekhotha et al., 2016), which could be caused by malfunctions of endothelial cells, subsequent insufficient angiogenesis, or abnormal development/regression of blood vessels (Andjelkovic et al., 2019; Lange et al., 2016; Theodorou and Boon, 2018). However, some farmers in developing countries, often do not receive adequate training on proper usage and potential toxic effects of pesticides. This can result in excessive exposures and residues in the environment that cause undesirable consequences (Fan et al., 2015; Gyenwali et al., 2017). According to a fact sheet, from World Health Organization (WHO), endothelial dysfunction and deficiencies in angiogenesis contributed to deaths of more than 6 million people globally, and accounted for nearly 10 % of total mortality, most of which occurred in low- and middle-income countries (Deaton et al., 2017). In 2011, Chinese farmers abused forchlorfenuron (CPPU), which is a growth-promoting agrochemical, to grow larger watermelons, which in some cases exploded. These exploding watermelons,

containing excessive residues of CPPU, were chopped up and fed to fish and pigs, which aroused concern of potential future hazards of CPPU in general populations of animals and humans that would consume these agricultural products (https://www.theguardian.com/world/2011/may/17/explodingwatermelons-chinese-farming).

Safety profiles and risk assessment of CPPU have been comprehensively reviewed (Arena et al., 2017). According to the US Environmental Protection Agency (US-EPA) pesticide fact sheet (https://www.epa.gov/sites/production/files/2015-04/documents/exhibit_b.pdf), CPPU is not necessarily harmless to the environment, or to animals and can, potentially affect humans. Potential hazards of CPPU to human and wildlife, including aquatic organisms, have been investigated by use of various experimental models. CPPU is known to inhibit dynamics of septin, a cytoskeletal protein, structure and function of which are highly conserved in eukaryote cells (Hu et al., 2008). In eukaryotes, CPPU inhibited fission of yeast cells budding with induction of ectopic septin structures (Iwase et al., 2004). CPPU has been reported to affect polymerization of septins, which reversibly paralyzed motility of a human blood fluke, *Schistosoma mansoni*, in specific stages of development (Zeraik et al., 2014). CPPU can cause cardio-toxicity in larval and adult zebrafish, as well as in mammalian cells even at concentrations less than 20 mg/L (Gong et al., 2019). Results of a 180-day, repeated-dose study, indicated CPPU disrupted production of steroid hormones and caused histopathological changes in ovaries of Sprague-Dawley rats (Bu et al., 2019). In a recent study, peripheral

blood-derived lymphocytes (PBLs), which were isolated from horses suffering from a form of eye inflammation, uveitis, that affects the middle layer of tissue in the eye wall (uvea). Thus, the horse is regarded as a spontaneous animal model for autoimmune uveitis in humans, were structural impairment of septin and an increase of migratory behavior were observed after exposure to CPPU (Wiedemann et al., 2020). Inhibition of proliferation of fission yeast cells, and mammalian cells by CPPU was attributed to reduced motility of ciliated protozoan in a mitochondria-dependent pathway, but independent of septin (Heasley et al., 2014). Recently, this has resulted in another concern for unanticipated adverse effects of CPPU especially in non-target organisms. Thus, potential threats of CPPU to growth and development of aquatic organisms or humans deserved further investigation.

Under most conditions, physiological functions of endothelial cells can be disrupted by oxidative stress, inflammatory reactions, and changes in the cytoskeleton (Gimbrone and Garcia-Cardena, 2016; Kleinstreuer et al., 2011). Therefore, CPPU was identified as a putative disruptor of the vascular system (Kleinstreuer et al., 2011); but there was no experimental evidence of such a causal relationship. During laboratory incubations of both soil and natural sediment-water systems under aerobic conditions in the dark, radio isotope labeled CPPU exhibited moderate persistence in acidic (pH 5.3) soil, to greater persistence at higher pH. The half-life of CPPU varied from 15.1 to 121.3 days (Sharma and Awasthi, 2003). The major transformation product of CPPU was 4-amino-2-chloropyridine (ACP), which accounted for 60% of the applied radioactivity (AR) in soil, 6% AR in water and 14% AR in sediment, and

was more persistent than its parent CPPU (Arena et al., 2017). Based on results of studies of natural sediments and laboratory investigations of aqueous photolysis, CPPU is resistant to photolysis and predicted to accumulate in sediments (Arena et al., 2017). Consequently, CPPU can frequently be detected in foods (Cao et al., 2019a; Meng et al., 2020; Shuiying et al., 2015; Xu et al., 2019) and waters (Liu et al., 2019) (Table 2). Also, CPPU has been reported to be accessible to and bioaccumulated by humans to concentrations that might cause adverse effects to agricultural workers (Shi et al., 2012; Toumi et al., 2018). Therefore, CPPU and its metabolite might remain in the circulatory system for extended periods. Since immature vasculature and endothelial system is vulnerable to insults by persistent toxicants (Cai et al., 2019), it was deemed a priority to examine effects of CPPU on endothelial function and vascular system, especially during early development.

Zebrafish are ideal animal models and widely adopted by pharmacologists and toxicologists to study vascular biology and ecotoxicity (Cassar et al., 2019; Rennekamp and Peterson, 2015; Schuermann et al., 2014). A human-derived cell line, human umbilical vein endothelial cell (HUVEC), which is sensitive to chemical insults, is a reliable cellular system to depict endothelial signaling transactions (Li et al., 2019a; Park et al., 2019b). Since the genetic control of vascular development between the zebrafish and humans is highly conserved, zebrafish *in vivo* and cultured mammalian endothelial cells *in vitro* are often used to complement each other to elucidate mechanisms underlying vascular development (Esser et al., 2017), to evaluate vascular toxicities of environmental toxicants (Wang et al., 2020; Zhong et

al., 2019b) or natural pharmaceutical products (Li et al., 2020; Yuan et al., 2018). In this study, potential toxicity of CPPU on the endothelial system of developing transgenic zebrafish expressing Tg(*fli-1*:eGFP) *in vivo*, and HUVEC *in vitro* was investigated. Also, the involvement of cellular signaling underlying endothelial toxicity of CPPU was further determined in HUVECs.

Materials and methods

Chemicals

Forchlorfenuron (CPPU, 1-(2-chloropyridin-4-yl)-3-phenylurea; CAS 68157-60-8; Figure 1D) of 99% (determined by HPLC), was obtained from Lin Guo fertilizer co. LTD (Guangzhou, China). Dimethyl sulfoxide (DMSO), 1-phenyl-2-thiourea (PTU), thiazolyl blue tetrazolium bromide (MTT), endothelial cell growth supplement (ECGS), paraformaldehyde (PFA), Phenylmethylsulfonyl fluoride (PMSF), tricaine, gelatin, heparin, fluorescein phalloidin and protease and phosphatase inhibitor cocktail were purchased from Sigma-Aldrich Co (St. Louis, MO, USA). DMEM, phosphate buffered saline (PBS), and penicillin-streptomycin (PS) were purchased from Gibco (Maryland, USA). Fetal bovine serum (FBS), trypsin-EDTA and TRIzol reagent were obtained from Invitrogen (Carlsbad, CA, USA). TB ® Premix Ex Taq™ II kit was purchased from TaKaRa (Dalian, China). Growth factor reduced (GFR) Matrigel™ was supplied by BD Biosciences (Bedford, MA). Vascular endothelial growth factor (VEGF) was bought from R&D System (Minneapolis, MN). Antibodies were purchased from cell signaling technology (Danvers, MA). All other chemicals of analytical grade were purchased from local sources.

172

173 **Maintenance of zebrafish and ethics statement**

174 Obtained from Zebrafish International Resource Center (University of Oregon,
175 USA), Wild type or transgenic zebrafish Tg(*fli-1*:eGFP), which allows easy imaging
176 of the endothelial cells and vascular compartment, were maintained in Institute of
177 Chinese Medical Sciences (ICMS), University of Macau (Liao et al., 2018). Detailed
178 information was included in supplemental section. Ethical approval
179 (UMARE-030-2017) for zebrafish studies was granted by the Animal Research Ethics
180 Committee, University of Macau (Gong et al., 2018).

181

182 **Chemical exposure and vascular structure observation**

183 Briefly, fertilized and normally developing embryos at 4 hpf were selected under
184 a microscope, after which, they were placed into a 24-well plate, with about 20
185 embryos per well containing 1 mL embryo medium. After treatment with various
186 concentrations of CPPU (0.025, 0.25, 2.5, 5, and 10 mg/L), at 56 or 72 hpf, the
187 common cardinal veins (CCVs), intersegmental vessels (ISVs) and sub-intestinal
188 vessels (SIVs) of larvae were observed and photographed under an Olympus DSU
189 (Disk Scanning Unit) confocal imaging system. Each treatment was performed in
190 triplicate.

191

192 **Quantitative real-time PCR analyses**

193 Zebrafish embryos at 4 hpf were exposed to 2.5, 5 or 10 mg CPPU/L for 4 days.

194 At 96 hpf, total RNA was extracted from 20 larvae per treatment group using TRIzol
195 reagent (Invitrogen, Carlsbad, CA, USA) according to the protocol from manufacturer.
196 cDNA in each treatment group was synthesized using SuperScript II Reverse
197 Transcriptase (Invitrogen) with random primers according to the protocol we
198 described previously (Liao et al., 2019). Real-time PCR was performed by Mx3005P
199 qPCR system (Agilent Technologies, Santa Clara, CA, USA) using the SYBR/TB
200 green ® Premix Ex Taq™ II kit (Takara, Dalian). The abundance of mRNA was
201 normalized to level of a housekeeping gene, elongation factor 1 α (*Ef1α*), and
202 expressed as a percentage of control (100%) for statistical analysis. Three replicates
203 were performed. Sequences of primers for amplification of each gene are shown in
204 Table 1 and Table S1.
205
206 **Cell culture, cell morphology and *in vitro* proliferation assay**
207 HUVEC cells were cultured in F-12 K complete media, which was supplemented
208 with 100 μg/ml heparin, 30 μg/ml ECGS, 10% FBS and 1% P/S, and incubated in a
209 humidified atmosphere with 5% CO_2 at 37 °C. Cells of early passage (2–8 passages)
210 were used in this study. When they had reached about 80% confluence, HUVECs
211 were dissociated and seeded into a 96-well plate at a density of 20000 cells/well. Cells
212 were grown at 37 °C for 24 h and exposed to a gradient of CPPU (2.5 – 80 mg/L) for
213 another 24 h. To study cytoskeleton, morphology of HUVECs was assessed by F-actin
214 (Fluorescein Phalloidin, isothiocyanate labeled) and nuclei (DAPI) staining. Briefly,
215 after an incubation of 24 h, HUVECs were fixed with 4% PFA at room temperature

for 15 min, followed by 5 min treatment of 0.2% triton. Morphologies of cells were observed by use of an IX73 microscope. Cell proliferation was assessed using the MTT method. At the end of incubation, MTT solution was added to each well, followed by incubation for 4 h in dark. Then, the medium and MTT were removed and formazan crystals were solubilized by addition of DMSO. Formazan crystals, solubilized into DMSO, were recorded at 570 nm with a multi-plate reader (SpectraMax M5 Microplate Reader; Molecular Devices, San Jose, CA, USA). Cell viability (regarded as proliferation) was calculated as a ratio (%) of optical density (OD) between treated and unexposed, control cells. The IC_{50} was calculated by GraphPad Prism 6 statistical software (San Diego, CA, USA). For this and following experiments of HUVECs, cells receiving 0.1% DMSO only served as a control and each treatment was performed in triplicate.

In vitro wound healing migration assay

HUVECs in growth medium were seeded into 24-well plates pre-coated with 0.1% gelatin and grown overnight to confluence. The monolayer cells were wounded by scratching with 200 μl pipette tips and washed with PBS to remove non-adherent cells. Completed medium together with concentrations of CPPU (5, 10 or 20 mg/L) were then added to wells. After 24 h incubation, images were taken at 0 h or 24 h by use of an IX73 microscope. The scratch area was evaluated by use of ImageJ software (MRI_Wound_Healing_Tool, on-line resources). The percentage of inhibition was expressed using control wells at 100%.

238

239 ***In vitro* Boyden chamber migration assay**

240 The Boyden chamber cell migration assay was accomplished by use of the
241 Real-time cell analysis (RTCA) instrument. Briefly, HUVECs at 2×10^4 cells / well
242 were added into a tailored 16-well plate, each well of which consisted of a golden
243 chamber pre-coated with 0.2% gelatin, in 100 μL cell culture medium containing 0, 5,
244 10 or 20 mg/L CPPU. After settled for 30 min, plate was placed in a xCELLigence
245 instrument at 37 °C, with 5% CO_2, in a humidified incubator. After incubation for 35
246 h, the cell index (CI) values were recorded and normalized at the first time point and
247 analysis were performed with the supplied RTCA software (version 1.2.1).

248

249 ***In vitro* tube formation assay**

250 Matrigel was thawed at 4 °C in a refrigerator overnight. Pre-chilled 96-well plates
251 were coated with 50 μl of Matrigel per well, incubated and solidified at 37 °C for 30
252 min. HUVECs at the density of 2×10^4 cells per well in completed F12-K medium
253 containing 5,10 or 20 mg/L CPPU or 0.1% DMSO were placed onto the layer of gel
254 and incubated for 2 h. The network formation was then visualized and imaged under
255 IX73 microscope at 10 magnification. Total length of tubes was quantified by ImageJ
256 Pro Plus software (angiogenesis analyzer tool). Values were obtained from three
257 experiments independently.

258

259 **Western blot analysis**

HUVECs were pre-treated with indicated concentrations of CPPU or 0.1% DMSO as control for 24 h before exposed to 50 ng/L of VEGF for 15 min (expect for one group receiving 0.1% DMSO). After that, cells were lysed for 20 min on ice with lysis buffer (Ripa with 1% saturated PMSF, 1% protease, and phosphatase inhibitor cocktail), and centrifuged. Protein concentrations in supernatants were measured using the Bradford Protein Assay Kit (Thermo fisher) and equalized before loading. After electrophoresed on 10% SDS-PAGE gel, proteins were transferred to polyvinylidene diuoride (PVDF) membranes and blocked with 5% non-fat milk. Immunoblot analysis was undertaken by incubation with antibody ERK1/2, phosphor-ERK1/2, MEK, phosphor-MEK, JNK, phosphor-JNK, FAK, phosphor-FAK, FLT, phosphor-FLT and GAPDH, respectively, overnight at 4 °C. After incubated with horseradish peroxidase-conjugated goat anti-rabbit or anti-mouse antibody (Beyotime, China), proteins were visualized by use of an ECL advanced Western blotting detection kit. Photos of protein bands were taken using Image Lab (Bio-Rad). Densitometry measurements of band intensity were performed using ImageJ. Detailed procedures were described in supplemental section.

Statistical analyses

All values were presented as means ± SD by use of a GraphPad Prism 6.0 software (GraphPad Software Inc., La Jolla, CA, USA). Data were investigated to determine if they met the assumptions of normality by use of the by using the Shapiro–Wilks test and for homogeneity of variance by use of Levene's test. If

necessary, data were log-transformed to approximate normality. Statistical significance of decrease/increase in fold of change was analyzed using one-way or two-way analysis of variance (ANOVA) followed by Dunnett multiple comparison test. The difference between two groups was determined by Student's t test. *P* values less than 0.05 were considered statistically significant.

Results

Effects of CPPU on rates of survival, hatching and body length of zebrafish

Rates of hatching and survival and body length of zebrafish embryos/larvae were affected by exposure to 0.025, 0.25, 2.5, 5, or 10 mg CPPU/L) (Figure 1B-D). Throughout the assay, exposure to 5 mg CPPU/L did not cause significant lethality of embryos. However, when the concentration of CPPU was greater than 5 mg/L, lethality was observed at 24 hpf and after longer exposures (Figure 1B). Specifically, at 96 hpf, 10 mg CPPU/L caused 60 % mortality of larvae. Exposure to CPPU also significantly decreased the rate of hatching of embryos in a dose- and time-dependent manner (Figure 1D). When exposed to 10 mg CPPU/L, at 72 hpf, only 40% of embryos hatched. At 96 hpf, mean body lengths of larvae were approximately 5, 10 and 15% less than that of the controls, after exposure to 2.5, 5 or 10 mg CPPU/L, respectively (Figure 1C).

CPPU impaired growth and formation in vascular structure of zebrafish

In this study, at 56 hpf, exposure to CPPU caused dose-dependent reduction in

304 areas of the CCVs and proportion of completed ISV (Figure 2A, 2B and 2D). In
305 detailed, zebrafish exposed to 0.025 mg CPPU/L exhibited significantly lesser CCVs
306 of about 30% compared to the controls (Figure 2A and 2B), while exposure to 2.5 mg
307 CPPU/L caused 40% reduction of completed ISVs. SIVs seem more sensitive to
308 CPPU treatment, 0.025 mg CPPU/L restrains its growth by 50% and 5 mg CPPU/L
309 almost totally abolished its formation. In brief, *in vivo*, exposure to CPPU hindered
310 the development of CCVs, ISVs and SIVs in a dose-dependent manner.
311
312 **CPPU affected some genes related to angiogenesis in zebrafish**
313 Exposure to 10 mg CPPU/L significantly up-regulated expressions of *flt-1* and
314 *kdr*, (Figure 3). No obvious alterations of expressions of mRNAs for other genes,
315 including *vegfa* and *kdrl* were observed at any of the concentrations of CPPU (Figure
316 3).
317
318 **Exposure to CPPU caused changes in the cytoskeleton of HUVECs**
319 Actin filaments are major components of cytoskeletons and are involved in
320 essential cell processes, such as motility and adherence, maintaining normal functions
321 of endothelial cells. Here, effects of exposure to CPPU on organization of actin
322 filaments in HUVECs were determined. Results of immunocytochemistry revealed
323 that exposure to CPPU significantly reduced volumes of cells (Figure 4A). Exposure
324 to CPPU also resulted in greater accumulations of actin in cells, in a dose-dependent
325 manner (Figure 4A, yellow arrowheads indicated).

Exposure to CPPU inhibited proliferation, tube formation and migration in HUVEC cells *in vitro*

Toxicities of CPPU to endothelial cells were further verified by exposing CPPU to human umbilical vein endothelial cells (HUVEC) *in vitro*. Mean survival curves were obtained by measuring HUVECs' viability using MTT assay, from which an IC_{50} value of 24.6 mg CPPU/L was estimated (Figure 4B). Formations of tubes is also required for angiogenesis and development of the vascular system. Structures of tubules in wells exposed to CPPU were incomplete with fewer branch points and shorter lengths of tubes (Figure 4D, yellow arrowheads indicated). Specifically, in HUVEC cells, CPPU was a potent inhibitor of tube formation, by about 90% at concentrations greater than 10 mg CPPU/L (Figure 4C).

Migrations of cells is a step in endothelial function and angiogenesis, inhibition of which could lead to insufficiency angiogenesis and cause dysfunction of the vasculature. CPPU inhibited horizontal migration in a scratch-wound assay with HUVEC cells, of between 30 and 60% inhibition when exposed to 10 or 20 mg/L, respectively (Figure 5A, 5B). Vertical migration of HUVEC cells, as determined by Boyden Chamber migration assay, was affected in a dose-dependent manner when exposed to CPPU (Figure 5C). Quantitative determination of migrated cells, measured as the impedance and expressed as the cell index, showed a significant inhibitory effect at or concentrations greater than 10 mg CPPU/L (Figure 5C). Results of *in vitro* exposures of HUVEC cells to CPPU, caused inhibition of key steps including

proliferation, migration and tube formation involved in angiogenesis, which suggested compromising of normal functions of vascular endothelial cells.

CPPU inhibited activation of FAK-MAPK pathway while increased phosphorylation of FLT-1 in VEGF treated HUVECs

Once initiated by activation of VEGF receptors by binding with its ligand, vascular endothelial growth factor receptor (such as FLT-1), FAK and its downstream MAPK signaling components such as MEK, ERK, and JNK can be activated to promote angiogenic processes, including cellular proliferation, migration and differentiation to form tube-like structure. Phosphorylation of FLT-1, FAK, MEK, ERK, and JNK in HUVEC cells were dramatically increased after being stimulated with VEGF (Figure 6-7). While treating HUVEC cells with CPPU, obviously inhibited VEGF mediated phosphorylation of FAK, MEK, ERK and JNK (Figure 6A and B, Figure 7A-D), with levels of total forms of each signaling pathway components almost unchanged (Figure 6A and 7A). These results suggested that CPPU inhibited the activation of FAK - MAPK signal transduction pathway. Moreover, CPPU significantly enhanced phosphorylation of FLT-1 in VEGF treated HUVEC cells (Figure 6A and 6C).

Discussion

As more and more etiologically unknown malfunctions of endothelial cells have occurred, consequent diseases, such as chronic wounds, ischemic attacks and

ischemic heart disease, have been more frequently diagnosed. Toxicities of several emerging environmental contaminants, including nanoparticles (Mostovenko et al., 2019), flame retardants, pesticides, had been determined to injure the vascular system of zebrafish or HUVECs, and a majority of which, such as nanoparticles, arsenic (Cai et al., 2019), arsenite (Xu et al., 2017), chromium (Cao et al., 2019b), microcystin-LR (Wang et al., 2019), triclosan (Zhang et al., 2019), paraquat (Pang et al., 2019), endosulfan (Zhang et al., 2017) and fipronil (Park et al., 2019b), can impair vascular endothelial function by causing apoptosis and oxidative stress. So far VEGF pathway has been regarded as the most important signaling for vascular development. Indeed, BDE-47 (Xing et al., 2018), BDE-99 (Zhong et al., 2019a), TDCPP (Zhong et al., 2019b), mixture of ioxynil and diethylstilbestrol (Li et al., 2019b), flufenoxuron (Park et al., 2019d), etoxazole (Park et al., 2019a) and bifenthrin (Park et al., 2019c) disturb the angiogenic process via suppressing expression of genes *flt-1*, *flt-4*, *kdr*, *kdrl*, *vegfc*, and *vegfa*, involved in VEGF–VEGF receptor (VEGFR) signaling pathway. There are four genes encoding VEGF receptors in zebrafish, and VEGFR-1 (*flt-1*) and VEGFR-2 (*flk-1*/*kdr* and *kdrl*) are mainly expressed in vascular endothelial cells, which mediated most of the angiogenic processes (Bussmann et al., 2008). Therefore, suppressing expressions of these genes or encoding proteins poses risks to vascular systems (Li et al., 2014). Contrarily, in zebrafish, CPPU induced no downregulation of VEGF related genes but significantly upregulated expression of mRNA for *flt-1* and *kdr* (Figure 3). We surmised that these upregulation were attributed to a feedback mechanism (Lam et al., 2012), implying an insufficient angiogenesis in zebrafish and

392 a compensation for such deficiency. In concordance, exposure to CPPU also
393 up-regulated expression of upstream effector FLT-1 (VEGFR-1) in HUVECs (Figure
394 6A and 6B), together suggested activation of compensatory angiogenic effects.

395 Angiogenesis requires tightly regulated homeostatic mechanisms (Li et al.,
396 2019a), and impaired induction of new sprouts, failures of coordination and direction
397 of endothelial cell proliferation, migration and lumen formation can cause toxicity to
398 endothelial cells (Carrillo et al., 2019; Zhang et al., 2018). Results of previous studies
399 have suggested that stimulation of VEGF promotes survival of endothelial cells,
400 proliferative and migratory behaviors, maintaining endothelial functions and
401 indispensable angiogenesis (Kuida and Boucher, 2004). Considering that CPPU
402 caused no interactions with VEGF receptors, further investigations into whether it
403 affected their downstream effectors or not were conducted. As downstream cascades
404 of VEGF receptor, mitogen activated protein kinase (MAPK, including ERK, p38 and
405 JNK) signaling is critical to VEGF-mediated migratory behaviors and angiogenic
406 processes. Among them, both ERK1/2 and JNK are key components in the cascade of
407 intracellular signaling pathways, which are found to be necessary for
408 VEGF-dependent survival, proliferation, migration and tube formation of endothelial
409 cells (Uchiba et al., 2004). Therefore, casual or chronic suppression of these
410 components, through environmental contamination or crop production agents, some
411 of them might not affect upstream receptors, should post potentially pose risks to the
412 vascular system (Sun et al., 2019; Tait et al., 2015). However, there have been few
413 studies focused on such relationship. Previous study indicated septin 7 protein

interacted with ERK at C-terminus tail and absence of septin 7 abolished the ability of ERK to promote migration. In this study, CPPU inhibited functions of septins and phosphorylation of downstream effectors (MEK/ERK/JNK) rather than VEGF receptors, resulting in defects of migratory behavior and causing toxicity to vessels. We also examined other downstream signaling after VEGF simulation, such as PI3K/Akt pathway (Sun et al., 2019), but found no alterations (Figure S1).

Normal cytoskeleton is involved in cellular processes including motility, adherence, vesicular traffic and cell division, thus is crucial in maintaining the endothelial function and healthy angiogenesis (Carrillo et al., 2019; Kleinstreuer et al., 2011). Recently, cylindrospermopsin was found to impair cytoskeleton of HUVECs and promote apoptosis by the Rho/ROCK signaling pathway, resulting in abnormal vascular development (Wang et al., 2020). Actin filaments are major components of cytoskeleton, which influence septin assembly into different structures, such as ring or filament. In contrast, septin was found to be associate with machinery of filamentous actin, and control actin polymerization. Dysfunctions of septin protein fail to promote polymerization of actin, thereby attenuate actin bundles, which causes destruction of cytoskeleton and irregular distribution/accumulation of actin. Since associations between actin and septin protein regulate cell adhesion and cell motility, paclitaxel (taxol), a well-known inhibitor of actin, injures cytoskeleton, angiogenesis and endothelial systems (Belotti et al., 1996). Knowing that CPPU is an inhibitor of septin (Sun et al., 2019), we did observe that CPPU reorganized the endothelial cytoskeleton, induced abnormal distribution of actin on the cell periphery, greatly lessened the cell

436 volume and cytoplasm, reduced cell adhesion and motility, which should trigger
437 toxicity to vascular system. Another important issue of cytoskeleton dynamic is focal
438 adhesion proteins, such as focal adhesion kinase (FAK), which has been described as
439 an important regulator of cell motility, adhesion and migration in endothelial cells
440 (Carrillo et al., 2019; Sun et al., 2019). In FAK gene knockout mice, early embryonic
441 lethality with extensive cardiovascular defects have been observed (Peng et al., 2008).
442 Our results also found reduced phosphorylation of FAK upon CPPU exposure,
443 strongly correlated toxicity of CPPU to dysfunctions of endothelial cytoskeleton and
444 adhesion proteins, rather than inhibition of VEGF receptors.

445 Currently the importance of maintaining vascular health, as well as ubiquity and
446 accessibility of vascular disruptors are becoming more and more apparent, and any
447 potential risks to blood vessels should be addressed. In general, plant growth
448 regulators and food additives were regarded as safe during their applications (Qian et
449 al., 2018). However, because of their potential bioaccumulation, their safe limits to
450 the environment and human beings are less than previously thought. Since CPPU is
451 extensively applied during modern agricultural production and accessible to humans,
452 through farming practices or fruits in market (Shi et al., 2012; Xu et al., 2019), its
453 environmental risks and toxicity to vascular systems are apparent. Although
454 assessments of hazards of CPPU and its metabolite ACP had identified low risk of
455 ecotoxicity in soil, surface water and sediment, their pesticidal activity in groundwater
456 is effective and toxicological relevance (Arena et al., 2017). Currently, based on
457 results of a 2-year study of mice, the agreed acceptable daily intake (ADI) is 0.05

mg/kg body mass (bm) per day, while the agreed acute reference dose (ARfD), based on skeletal variations in the rabbit teratology study, is 0.5 mg/kg bm and the acceptable operator exposure level (AOEL), based on results of a 90-day study of rats is 0.16 mg/kg bm per day, and the agreed acute acceptable operator exposure level (AAOEL) is 0.5 mg/kg bm (Arena et al., 2017). Although further details on toxic potency to mammals are still needed, for CPPU, its excessive residues have been detected in different fruits in china (Shuiying et al., 2015), which might be attributed to lax and mistaken agricultural practices. During mixing, loading, spraying, cleaning up spills, maintaining equipment and when entering treated areas, workers might be exposed to CPPU (Arena et al., 2017). Considering CPPU treatment potentially caused exploding of watermelons, and was detrimental to the cardiovascular system of zebrafish, even humans (Gong et al., 2019), its agricultural practice should be normalized, and its residues should be strict supervision. In addition, use of face shields or goggles, gloves, and protective clothing is required when opening the container and preparing spray. Applications and risk assessment of CPPU were well characterized on kiwi fruits and grapes but needed completion regarding watermelon. Although there is still a huge data gap between human and experimental animals, adverse findings in animal species are assumed to represent potential effects in humans. Study on zebrafish do reveal potential risks to ecology, and likely, human hazard (Cassar et al., 2019; Rennekamp and Peterson, 2015).

Conclusions

In summary, effects involving disorganization of cytoskeleton and FAK-MAPK signaling pathway underlying vascular toxicity of CPPU was observed. Although CPPU exhibited no inhibition to VEGF receptor and its encoding genes in zebrafish, it disrupted endothelial cell cytoskeleton with inhibition of downstream FAK-MAPK signaling in HUVECs. In addition, this study underscores putative hazards of cytoskeletal disrupters and proposes adverse potential degradation of water quality by CPPU runoff associated with risks, including environmental safety by its ubiquitous exposure and human health by the consumption of the contaminated fruits or the fish products in the contaminated aquatic system.

Potential conflicts of interest

The authors declare no conflict of interest.

Acknowledgements

Research at University of Macau was funded by The Science and Technology Development Fund, Macau SAR (File no. 0058/2019/A1 and 0016/2019/AKP), and University of Macau (MYRG2019-00105-ICMS). Prof Giesy supported by the Canada Research Chairs Program of the Natural Sciences and Engineering Research Council of Canada (NSERC) and a distinguished visiting professorship from the Department of Environmental Sciences, Baylor University, Waco, Texas, USA.

Figure Legends

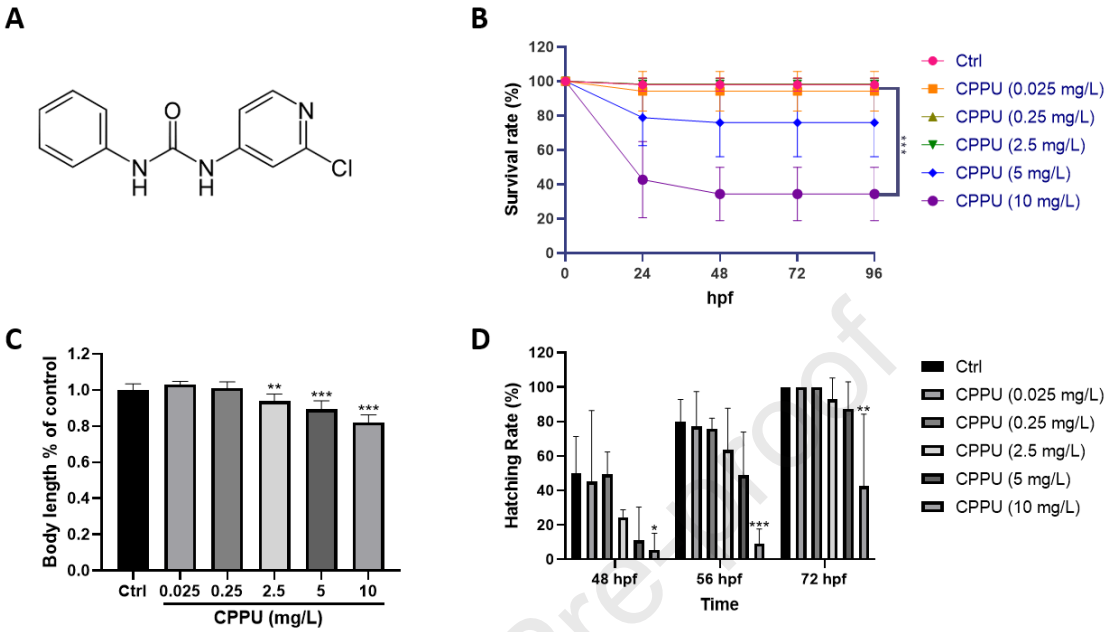

Figure 1. Effects of exposure of zebrafish embryos to CPPU for 96 h. (A) Chemical structure of CPPU. (B) Survival rate at 24, 48, 72 and 96 hpf, (C) Body length at 96 hpf and (D) Hatching rate at 48, 56, 72 hpf were recorded after different concentrations of CPPU treatment (0.025, 0.25, 2.5, 5 and 10 mg/L). Data are plotted as means ± SD (n = 12-18). Each treatment was performed in triplicate. *, $P < 0.05$, **, $P < 0.01$ and ***, $P < 0.001$ versus blank control group.

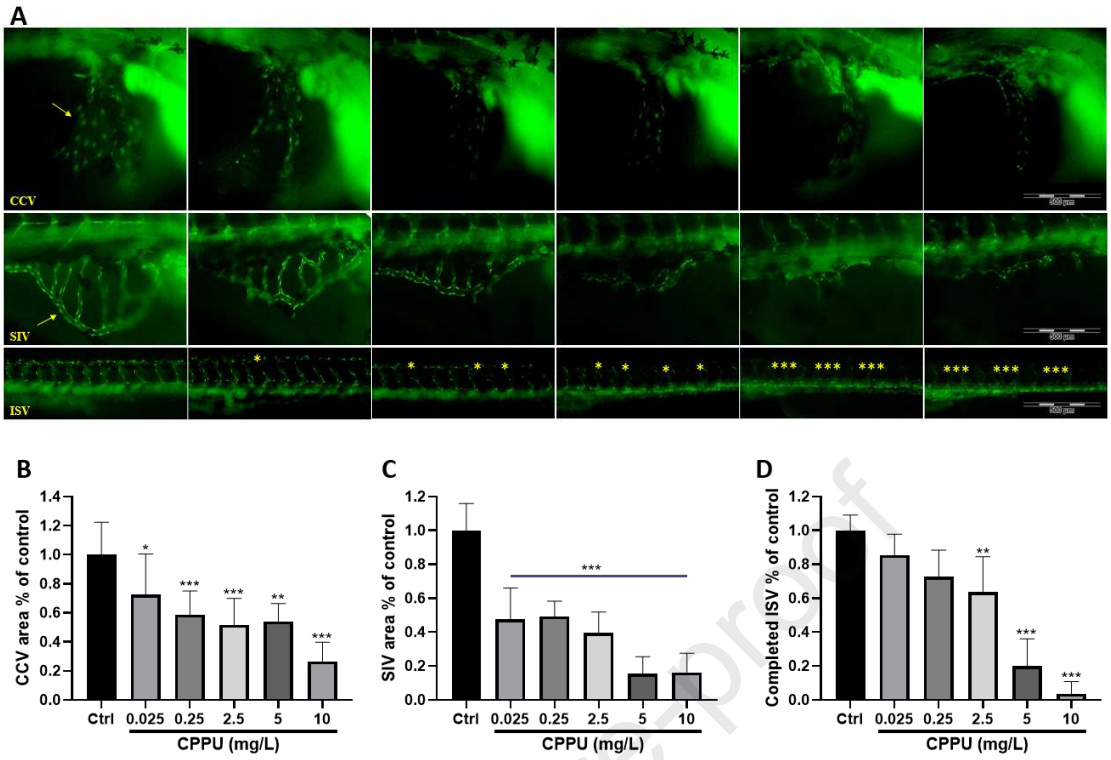

Figure 2. Effects of CPPU on vascular development of transgenic zebrafish Tg(*fli-1*:eGFP). (A) Representative images of CCVs, SIVs and ISVs after various drug treatments at 56, 72, 56 hpf. Yellow arrows indicate structures of CCVs and SIVs, and yellow stars indicate uncompleted ISVs. (B-D) CCV, SIV vascularized areas and completed ISV proportion were quantified in control and various exposures of zebrafish larvae to CPPU. Data are presented as mean ± SD. n = 12–18. Each treatment was performed in triplicate. *, $P < 0.05$ **, $P < 0.01$ and ***, $P < 0.001$ versus blank control group.

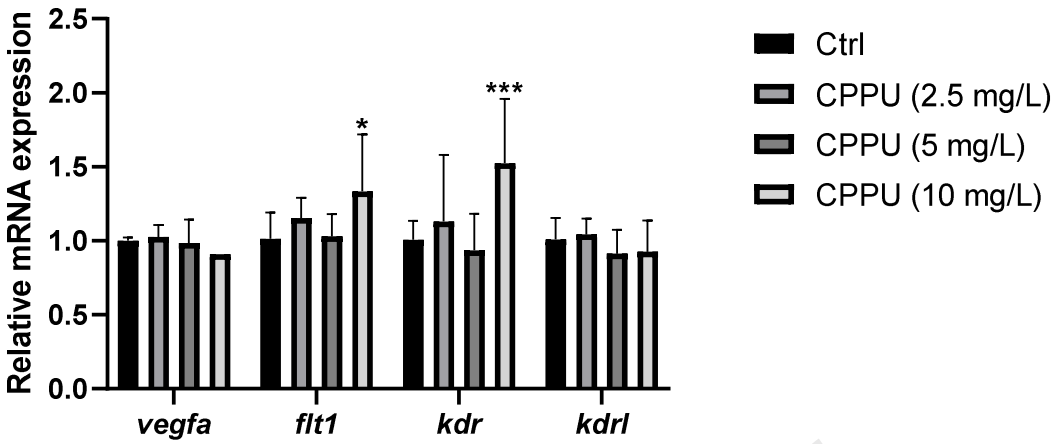

Figure 3. CPPU exposure altered expression of genes related to vascular growth and remodeling. Expression of mRNA for *vegfa*, *flt1*, *kdr* and *kdrl* in zebrafish larvae exposed to vehicle control, 2.5, 5 and 10 mg/L CPPU at 96 hpf. Data are presented as mean ± SD. n = 3. *, $P < 0.05$ and ***, $P < 0.001$ versus blank control group.

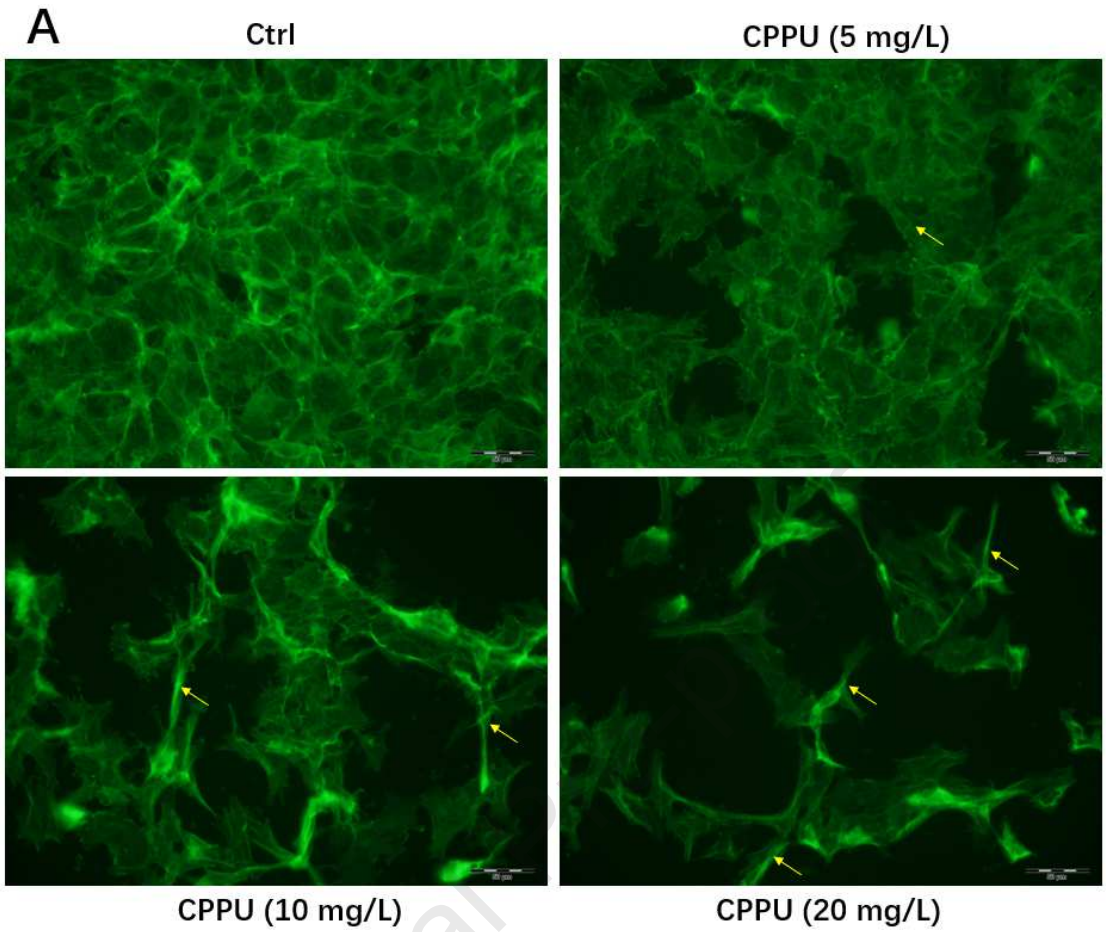
A
Ctrl
CPPU (5 mg/L)
CPPU (10 mg/L)
CPPU (20 mg/L)

533

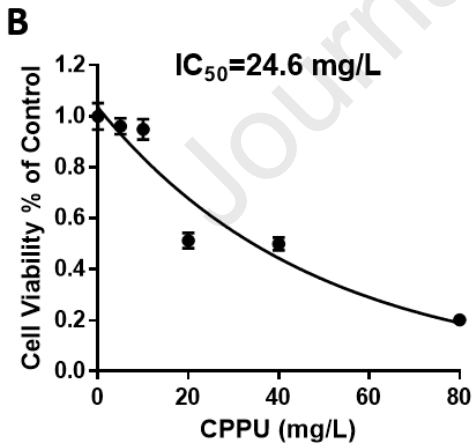
B
IC50=24.6 mg/L
Cell Viability % of Control
1.2
1.0
0.8
0.6
0.4
0.2
0.0
0
20
40
60
80
CPPU (mg/L)

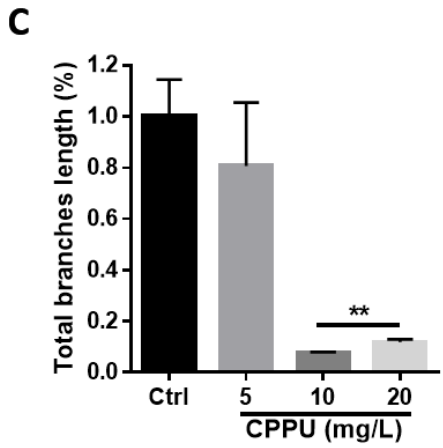
C
Total branches length (%)
1.2
1.0
0.8
0.6
0.4
0.2
0.0
**
Ctrl
5
10
20
CPPU (mg/L)

534

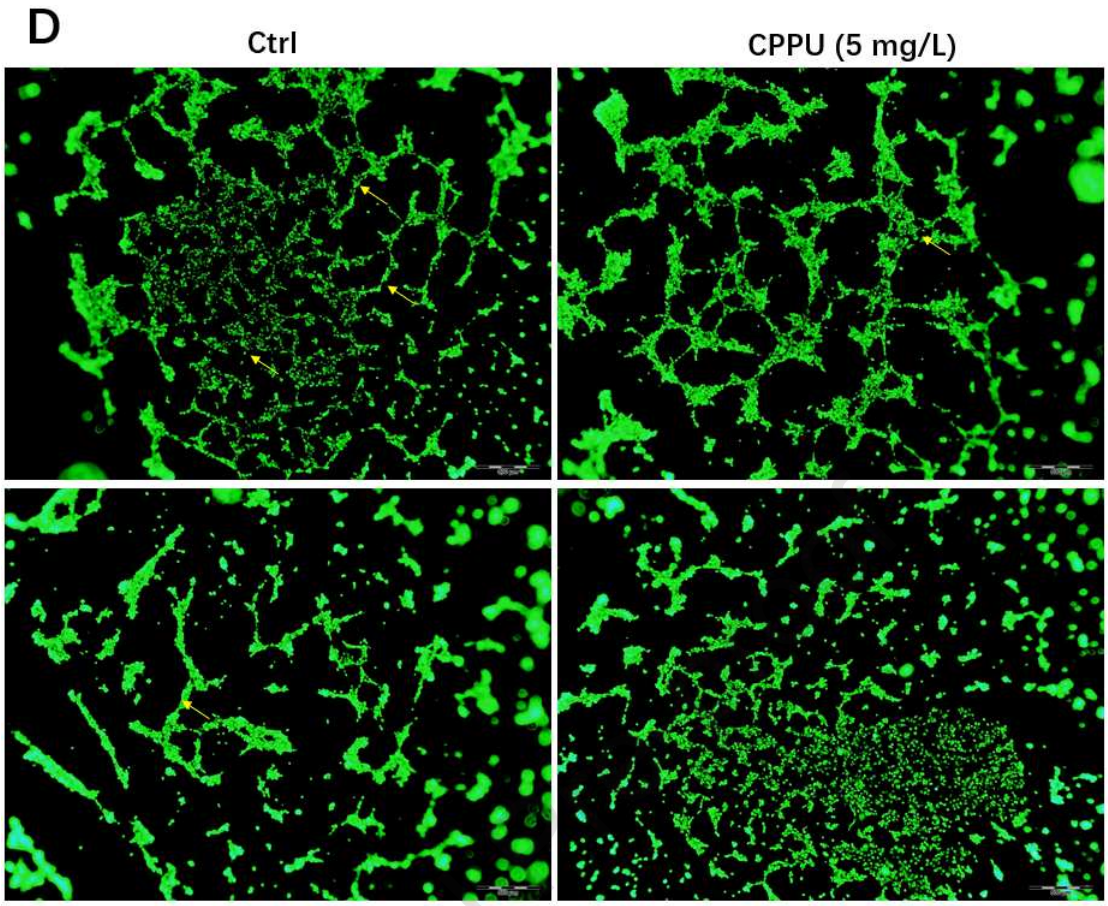

Figure 4. CPPU-induced rearrangement of cytoskeleton, inhibited proliferation, and formation of tubular-like structures in HUVECs *in vitro*. (A) Representative photographs of fluorescence immunocytochemistry of actin in control (DMSO) or treated with CPPU for 24 h. (B) Representative survival curve of HUVECs in presence of increasing concentrations of CPPU for 24 h. IC_{50} = 24.6 mg/L. Values are means ± SD. n = 3. The IC_{50} was calculated using Prism 6 with nonlinear regression (curve fitting). (C) Quantitative analysis of the total length of branches as percentage compared to lengths in untreated controls. (D) Representative photographs of HUVECs tube formation on Matrigel at various concentrations of CPPU. Data are presented as mean ± SD. n = 3. **, $P < 0.01$ versus blank control group. Yellow arrows indicate accumulation of actin and tubular branches, respectively.

547

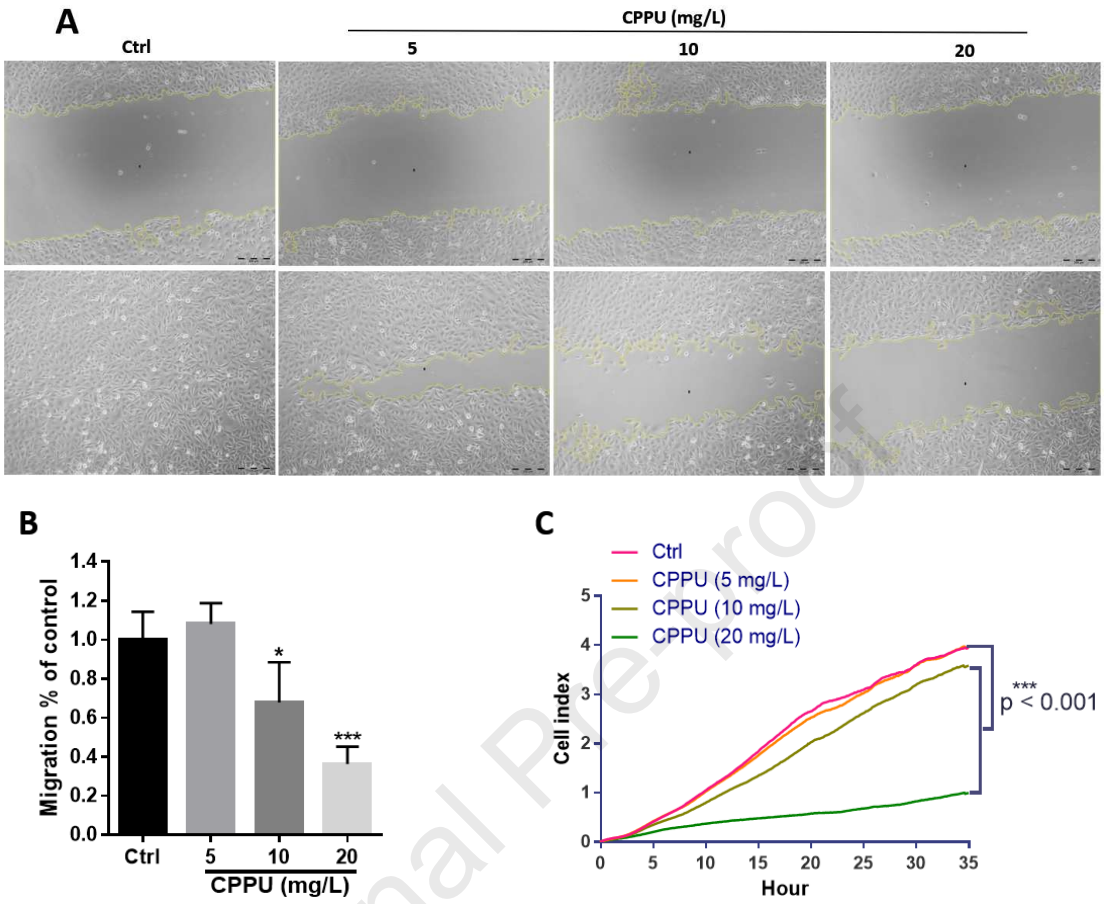

548

549

550 **Figure 5. I**nhibition of migration in HUVECs by *in vitro* exposure to CPPU. (A) Representative
551 photographs of migration of HUVECs (wound healing assay) at 0 or 8 h when exposed to 5, 10 or
552 20 mg CPPU/L or control (DMSO) conditions. (B) Quantitative analysis of migration areas in the
553 wound healing assay after 8 h at each concentration. (C) Changes in impedance across HUVECs
554 monolayer were measured by the xCELLigence Real-time cell analysis (RTCA) system to
555 evaluate vertical migration ability (Boyden Chamber assay) after exposure to CPPU for 35 h. Cell
556 Index values were represented as numbers of migrated cells. Data are presented as mean ± SD. n =
557 3. *, $P < 0.05$ and ***, $P < 0.001$ versus blank control group.

558

559

560

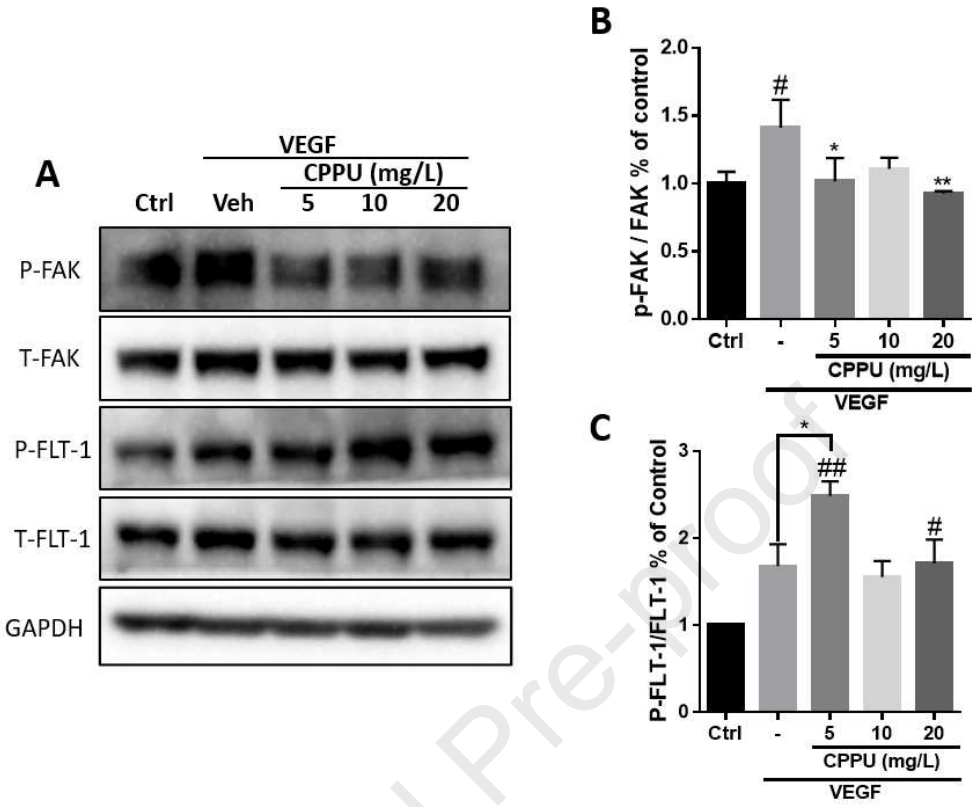

561

562 **Figure 6.** CPPU decreased phosphorylated FAK while increasing phosphorylated levels of FLT-1

563 in VEGF stimulated HUVECs *in vitro.* (A) Representative Western blot images of phosphorylated

564 and total forms of FAK and FLT-1 1 in HUVECs control (DMSO) or treated with CPPU for 24 h.

565 Quantification of phosphorylated FAK relative to total FAK (B), phosphorylated FLT-1 relative to

566 total FLT-1 signal (C) in Western-blot photographs. Data are presented as mean ± SD. n = 3. #, P <

567 0.05; ##, P < 0.01 versus blank control group. *, P < 0.05 and **, P < 0.01 versus vehicle (VEGF

568 treatment) group.

569

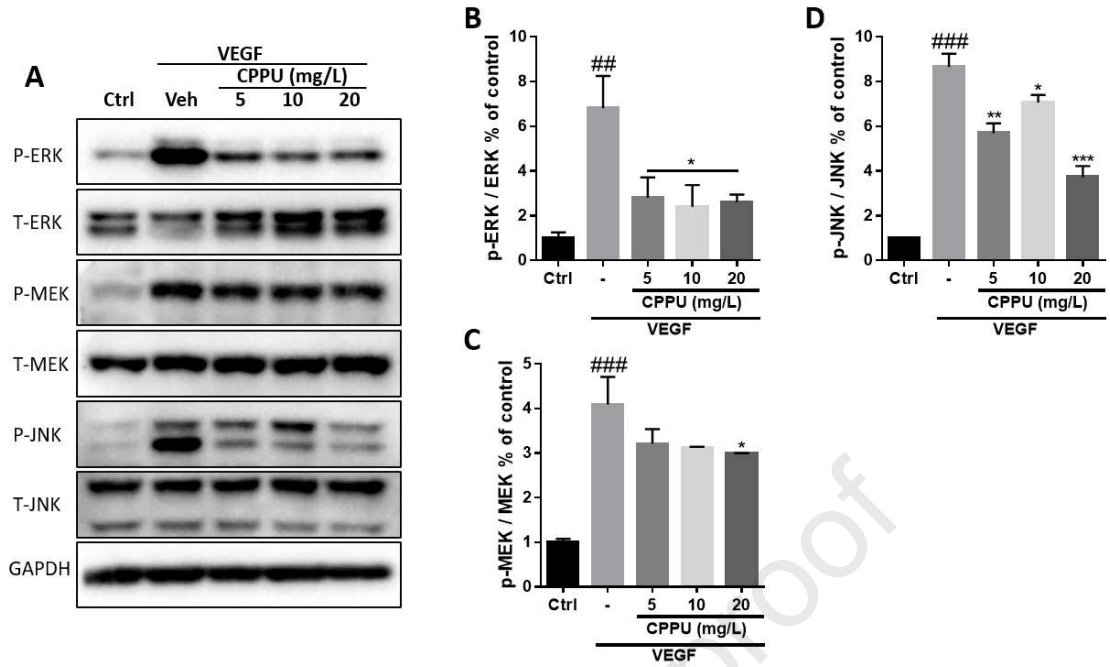

Figure 7. CPPU inhibited the MAPK signal transduction pathway in VEGF stimulated HUVECs *in vitro*. (A) Representative Western blot images of phosphorylated and total forms of ERK, MEK, JNK in HUVECs control (DMSO) or treated with CPPU for 24 h. Quantification of phosphorylated (B) ERK, (C) MEK, (D) JNK relative to their respectively total forms in Western-blot photographs. Data are presented as mean ± SD. n = 3. ##, $P < 0.01$ and ###, $P < 0.001$ versus blank control group. *, $P < 0.05$; **, $P < 0.01$ and ***, $P < 0.001$ versus vehicle (VEGF treatment) group.

585

586 Table 1. Primers used in quantitative RT-PCR.

Prime	Sequence
vegfa forward	5’-TGTAATGATGAGGCGCTCGAA-3’
vegfa reverse	5’-AGGCTCACAGTGGTTTTCTT-3’
flt-1 forward	5’-AACTCACAGACCAGTGAACAAGATC-3’
flt-1 reverse	5’-GCCCTGTAACGTGTGCACTAAA-3’
kdr forward	5’-CAAGTAACTCGTTTTCTCAACCTAAGC-3’
kdr reverse	5’-GGTCTGCTACACAACGCATTATAAC-3’
kdrl forward	5’-GACCATAAAACAAGTGAGGCAGAAG- 3’
kdrl reverse	5’-CTCCTGGTTTGACAGAGCGATA-3’
elfα forward	5’-GCTCAAACATGGGCTGGTTC-3’
elfα reverse	5’-AGGGCATCAAGAAGAGTAGTACCG-3’

587

588 Table 2. Summary of concentrations of CPPU detected in various matrices.

Samples	Sample with CPPU residue / Total samples	Concentrations levels	References
Cucumber	9/20	2.0-23.5 mg/kg (mg/L)	Cao et al., 2019a; Meng et al., 2020
Watermelon	7/20	0.125-10.8 mg/kg (mg/L)	Meng et al., 2020; Shuiying et al., 2015
Bean sprouts	5/20	0.79-7.27 μg/kg (μg/L)	Cao et al., 2019a;
Water [a]	4/20	0.214-0.725	Liu et al., 2019b

	ng/L

a. Bottom water and surface water of Jiulong River Estuary

References

Andjelkovic, A.V., Xiang, J., Stamatovic, S.M., Hua, Y., Xi, G., Wang, M.M., Keep, R.F., 2019. Endothelial Targets in Stroke: Translating Animal Models to Human. Arterioscler Thromb Vasc Biol 39, 2240-2247.

Arena, M., Auteri, D., Barmaz, S., Bellisai, G., Brancato, A., Brocca, D., Bura, L., Byers, H., Chiusolo, A., Court Marques, D., Crivellente, F., De Lentdecker, C., De Maglie, M., Egsmose, M., Erdos, Z., Fait, G., Ferreira, L., Goumenou, M., Greco, L., Ippolito, A., Istace, F., Jarrah, S., Kardassi, D., Leuschner, R., Lythgo, C., Magrans, J.O., Medina, P., Miron, I., Molnar, T., Nougadere, A., Padovani, L., Parra Morte, J.M., Pedersen, R., Reich, H., Sacchi, A., Santos, M., Serafimova, R., Sharp, R., Stanek, A., Streissl, F., Sturma, J., Szentes, C., Tarazona, J., Terron, A., Theobald, A., Vagenende, B., Verani, A., Villamar-Bouza, L., 2017. Peer review of the pesticide risk assessment of the active substance forchlorfenuron. EFSA Journal 15.

Barmentlo, S.H., Schrama, M., Hunting, E.R., Heutink, R., van Bodegom, P.M., de Snoo, G.R., Vijver, M.G., 2018. Assessing combined impacts of agrochemicals: Aquatic macroinvertebrate population responses in outdoor mesocosms. Sci Total Environ 631-632, 341-347.

Belotti, D., Vergani, V., Drudis, T., Borsotti, P., Pitelli, M.R., Viale, G., Giavazzi, R., Taraboletti, G., 1996. The microtubule-affecting drug paclitaxel has antiangiogenic activity. Clinical Cancer Research 2, 1843-1849.

Bu, Q., Wang, X., Xie, H., Zhong, K., Wu, Y., Zhang, J., Wang, Z., Gao, H., Huang, Y., 2019. 180 Day Repeated-Dose Toxicity Study on Forchlorfenuron in Sprague-Dawley Rats and Its

610 Effects on the Production of Steroid Hormones. J Agric Food Chem 67, 10207-10213.

611 Bussmann, J., Lawson, N., Zon, L., Schulte-Merker, S., Zebrafish Nomenclature, C., 2008.
612 Zebrafish VEGF receptors: a guideline to nomenclature. PLoS Genet 4, e1000064.

613 Cai, Z., Zhang, Y., Zhang, Y., Miao, X., Li, S., Yang, H., Ling, Q., Hoffmann, P.R., Huang, Z.,
614 2019. Use of a Mouse Model and Human Umbilical Vein Endothelial Cells to Investigate the
615 Effect of Arsenic Exposure on Vascular Endothelial Function and the Associated Role of
616 Calpains. Environ Health Perspect 127, 77003.

617 Cao, J., Li, R., Liang, S., Li, J., Xu, Q., Wang, C., 2019a. Simultaneous extraction of four plant
618 growth regulators residues in vegetable samples using solid phase extraction based on
619 thiol-functionalized nanofibers mat. Food Chem, 125859.

620 Cao, X., Wang, S., Bi, R., Tian, S., Huo, Y., Liu, J., 2019b. Toxic effects of Cr(VI) on the bovine
621 hemoglobin and human vascular endothelial cells: Molecular interaction and cell damage.
622 Chemosphere 222, 355-363.

623 Carrillo, P., Martinez-Poveda, B., Medina, M.A., Quesada, A.R., 2019. The strigolactone
624 analog GR-24 inhibits angiogenesis in vivo and in vitro by a mechanism involving cytoskeletal
625 reorganization and VEGFR2 signalling. Biochem Pharmacol 168, 366-383.

626 Carvalho, F.P., 2017. Pesticides, environment, and food safety. Food and Energy Security 6,
627 48-60.

628 Cassar, S., Adatto, I., Freeman, J.L., Gamse, J.T., Iturria, I., Lawrence, C., Muriana, A.,
629 Peterson, R.T., Van Cruchten, S., Zon, L.I., 2019. Use of Zebrafish in Drug Discovery
630 Toxicology. Chem Res Toxicol.

631 Curl, C.L., Beresford, S.A., Fenske, R.A., Fitzpatrick, A.L., Lu, C., Nettleton, J.A., Kaufman,

J.D., 2015. Estimating pesticide exposure from dietary intake and organic food choices: the Multi-Ethnic Study of Atherosclerosis (MESA). Environ Health Perspect 123, 475-483.

Deaton, C., Froelicher, E.S., Wu, L.H., Ho, C., Shishani, K., Jaarsma, T., 2017. The Global Burden of Cardiovascular Disease. European Journal of Cardiovascular Nursing 10, S5-S13.

Esser, J.S., Charlet, A., Schmidt, M., Heck, S., Allen, A., Lother, A., Epting, D., Patterson, C., Bode, C., Moser, M., 2017. The neuronal transcription factor NPAS4 is a strong inducer of sprouting angiogenesis and tip cell formation. Cardiovascular Research 113, 222-223.

Fan, L., Niu, H., Yang, X., Qin, W., Bento, C.P., Ritsema, C.J., Geissen, V., 2015. Factors affecting farmers' behaviour in pesticide use: Insights from a field study in northern China. Sci Total Environ 537, 360-368.

Gimbrone, M.A., Jr., Garcia-Cardena, G., 2016. Endothelial Cell Dysfunction and the Pathobiology of Atherosclerosis. Circ Res 118, 620-636.

Gong, G., Jiang, L., Lin, Q., Liu, W., He, M.F., Zhang, J., Feng, F., Qu, W., Xie, N., 2018. In vivo toxic effects of 4-methoxy-5-hydroxy-canthin-6-one in zebrafish embryos via copper dyshomeostasis and oxidative stress. Comp Biochem Physiol C Toxicol Pharmacol 204, 79-87.

Gong, G., Kam, H., Tse, Y., Lee, S.M., 2019. Cardiotoxicity of forchlorfenuron (CPPU) in zebrafish (Danio rerio) and H9c2 cardiomyocytes. Chemosphere 235, 153-162.

Gyenwali, D., Vaidya, A., Tiwari, S., Khatiwada, P., Lamsal, D.R., Giri, S., 2017. Pesticide poisoning in Chitwan, Nepal: a descriptive epidemiological study. BMC Public Health 17, 619.

Heasley, L.R., Garcia, G., Mcmurray, M.A., 2014. Off-Target Effects of the Septin Drug Forchlorfenuron on Nonplant Eukaryotes. Eukaryotic Cell 13, 1411-1420.

654 Hu, Q., Nelson, W.J., Spiliotis, E.T., 2008. Forchlorfenuron alters mammalian septin assembly,
655 organization, and dynamics. J Biol Chem 283, 29563-29571.
656 Iwase, M., Okada, S., Oguchi, T., Toh-e, A., 2004. Forchlorfenuron, a phenylurea cytokinin,
657 disturbs septin organization in Saccharomyces cerevisiae. Genes & Genetic Systems 79,
658 199-206.
659 Kim, S.A., Kim, K.S., Lee, Y.M., Jacobs, D.R., Lee, D.H., 2015. Associations of organochlorine
660 pesticides and polychlorinated biphenyls with total, cardiovascular, and cancer mortality in
661 elders with differing fat mass. Environ Res 138, 1-7.
662 Kleinstreuer, N.C., Judson, R.S., Reif, D.M., Sipes, N.S., Singh, A.V., Chandler, K.J.,
663 DeWoskin, R., Dix, D.J., Kavlock, R.J., Knudsen, T.B., 2011. Environmental impact on
664 vascular development predicted by high-throughput screening. Environmental health
665 perspectives 119, 1596-1603.
666 Kuida, K., Boucher, D.M., 2004. Functions of MAP kinases: insights from gene-targeting
667 studies. J Biochem 135, 653-656.
668 Lam, I.K., Alex, D., Wang, Y.H., Liu, P., Liu, A.L., Du, G.H., Lee, S.M., 2012. In vitro and in vivo
669 structure and activity relationship analysis of polymethoxylated flavonoids: identifying
670 sinensetin as a novel antiangiogenesis agent. Molecular Nutrition & Food Research 56,
671 945-956.
672 Lange, C., Storkebaum, E., de Almodovar, C.R., Dewerchin, M., Carmeliet, P., 2016. Vascular
673 endothelial growth factor: a neurovascular target in neurological diseases. Nat Rev Neurol 12,
674 439-454.
675 Li, J., Li, F., Tang, F., Zhang, J., Li, R., Sheng, D., Lee, S.M., Zhou, G.C., Leung, G.P., 2019a.

AGS-30, an andrographolide derivative, suppresses tumor angiogenesis and growth in vitro and in vivo. Biochem Pharmacol 171, 113694.

Li, J., Tang, F., Li, R., Chen, Z., Lee, S.M., Fu, C., Zhang, J., Leung, G.P., 2020. Dietary compound glycyrrhetinic acid suppresses tumor angiogenesis and growth by modulating antiangiogenic and proapoptotic pathways in vitro and in vivo. Journal of Nutritional Biochemistry 77, 108268.

Li, S., Dang, Y.Y., Oi Lam Che, G., Kwan, Y.W., Chan, S.W., Leung, G.P., Lee, S.M., Hoi, M.P., 2014. VEGFR tyrosine kinase inhibitor II (VRI) induced vascular insufficiency in zebrafish as a model for studying vascular toxicity and vascular preservation. Toxicol Appl Pharmacol 280, 408-420.

Li, Y.F., Canario, A.V.M., Power, D.M., Campinho, M.A., 2019b. Ioxynil and diethylstilbestrol disrupt vascular and heart development in zebrafish. Environ Int 124, 511-520.

Liao, Q., Gong, G., Siu, S.W.I., Wong, C.T.T., Yu, H., Tse, Y.C., Radis-Baptista, G., Lee, S.M., 2018. A Novel ShK-Like Toxic Peptide from the Transcriptome of the Cnidarian Palythoa caribaeorum Displays Neuroprotection and Cardioprotection in Zebrafish. Toxins (Basel) 10.

Liao, Q., Li, S., Siu, S.W.I., Morlighem, J.R.L., Wong, C.T.T., Wang, X., Radis-Baptista, G., Lee, S.M., 2019. Novel neurotoxic peptides from Protopalythoa variabilis virtually interact with voltage-gated sodium channel and display anti-epilepsy and neuroprotective activities in zebrafish. Arch Toxicol 93, 189-206.

Lind, L., Lind, P.M., 2012. Can persistent organic pollutants and plastic-associated chemicals cause cardiovascular disease? J Intern Med 271, 537-553.

Liu, Z., Qi, P., Wang, J., Wang, Z., Di, S., Xu, H., Zhao, H., Wang, Q., Wang, X., Wang, X.,

2019. Development, validation, comparison, and implementation of a highly efficient and effective method using magnetic solid-phase extraction with hydrophilic-lipophilic-balanced materials for LC-MS/MS analysis of pesticides in seawater. Sci Total Environ, 135221.

Meng, X., Zhai, Y., Yuan, W., Lv, Y., Lv, Q., Bai, H., Niu, Z., Xu, W., Ma, Q., 2020. Ambient ionization coupled with a miniature mass spectrometer for rapid identification of unauthorized adulterants in food. Journal of Food Composition and Analysis 85.

Mostovenko, E., Young, T., Muldoon, P.P., Bishop, L., Canal, C.G., Vucetic, A., Zeidler-Erdely, P.C., Erdely, A., Campen, M.J., Ottens, A.K., 2019. Nanoparticle exposure driven circulating bioactive peptidome causes systemic inflammation and vascular dysfunction. Part Fibre Toxicol 16, 20.

Pang, L., Deng, P., Liang, Y.-d., Qian, J.-y., Wu, L.-C., Yang, L.-l., Yu, Z.-p., Zhou, Z., 2019. Lipoic acid antagonizes paraquat-induced vascular endothelial dysfunction by suppressing mitochondrial reactive oxidative stress. Toxicology Research 8, 918-927.

Park, H., Lee, J.Y., Park, S., Song, G., Lim, W., 2019a. Developmental toxicity and angiogenic defects of etoxazole exposed zebrafish (Danio rerio) larvae. Aquat Toxicol 217, 105324.

Park, H., Lee, J.Y., Park, S., Song, G., Lim, W., 2019b. Developmental toxicity of fipronil in early development of zebrafish (Danio rerio) larvae: Disrupted vascular formation with angiogenic failure and inhibited neurogenesis. J Hazard Mater, 121531.

Park, S., Lee, J.Y., Park, H., Song, G., Lim, W., 2019c. Bifenthrin induces developmental immunotoxicity and vascular malformation during zebrafish embryogenesis. Comp Biochem Physiol C Toxicol Pharmacol 228, 108671.

Park, S., Lee, J.Y., Park, H., Song, G., Lim, W., 2019d. Toxic effects of flufenoxuron on

development and vascular formation during zebrafish embryogenesis. Aquat Toxicol 216, 105307.

Peng, X., Wu, X., Druso, J.E., Wei, H., Park, A.Y.-J., Kraus, M.S., Alcaraz, A., Chen, J., Chien, S., Cerione, R.A., 2008. Cardiac developmental defects and eccentric right ventricular hypertrophy in cardiomyocyte focal adhesion kinase (FAK) conditional knockout mice. Proceedings of the National Academy of Sciences 105, 6638-6643.

Qian, C., Ren, N., Wang, J., Xu, Q., Chen, X., Qi, X., 2018. Effects of exogenous application of CPPU, NAA and GA4+7 on parthenocarpy and fruit quality in cucumber (Cucumis sativus L.). Food Chem 243, 410-413.

Rennekamp, A.J., Peterson, R.T., 2015. 15 years of zebrafish chemical screening. Curr Opin Chem Biol 24, 58-70.

Rundlof, M., Lundin, O., 2019. Can Costs of Pesticide Exposure for Bumblebees Be Balanced by Benefits from a Mass-Flowering Crop? Environ Sci Technol.

Schuermann, A., Helker, C.S., Herzog, W., 2014. Angiogenesis in zebrafish. Semin Cell Dev Biol 31, 106-114.

Sekhotha, M.M., Monyeki, K.D., Sibuyi, M.E., 2016. Exposure to Agrochemicals and Cardiovascular Disease: A Review. Int J Environ Res Public Health 13, 229.

Sharma, D., Awasthi, M.D., 2003. Behaviour of forchlorfenuron residues in grape, soil and water. Chemosphere 50, 589-594.

Shi, X., Jin, F., Huang, Y., Du, X., Li, C., Wang, M., Shao, H., Jin, M., Wang, J., 2012. Simultaneous determination of five plant growth regulators in fruits by modified quick, easy, cheap, effective, rugged, and safe (QuEChERS) extraction and liquid chromatography-tandem

742 mass spectrometry. J Agric Food Chem 60, 60-65.

743 Shuiying, R., Yun, G., Shun, F., Yi, L., 2015. Simultaneous determination of 10 plant growth
744 promoters in fruits and vegetables with a modified QuEChERS based liquid chromatography
745 tandem mass spectrometry method. Analytical Methods 7, 9130-9136.

746 Solomon, K., Giesy, J., Jones, P., 2000. Probabilistic risk assessment of agrochemicals in the
747 environment. Crop Protection 19, 649-655.

748 Sun, L., Cao, X., Lechuga, S., Feygin, A., Naydenov, N.G., Ivanov, A.I., 2019. A Septin
749 Cytoskeleton-Targeting Small Molecule, Forchlorfenuron, Inhibits Epithelial Migration via
750 Septin-Independent Perturbation of Cellular Signaling. Cells 9.

751 Tait, S., Tassinari, R., Maranghi, F., Mantovani, A., 2015. Bisphenol A affects placental layers
752 morphology and angiogenesis during early pregnancy phase in mice. J Appl Toxicol 35,
753 1278-1291.

754 Theodorou, K., Boon, R.A., 2018. Endothelial Cell Metabolism in Atherosclerosis. Front Cell
755 Dev Biol 6, 82.

756 Toumi, K., Joly, L., Vleminckx, C., Schiffers, B., 2018. ASSESSMENT OF BELGIAN
757 FLORISTS EXPOSURE TO PESTICIDE RESIDUES. Communications in Agricultural and
758 Applied Biological Sciences 83.

759 Uchiba, M., Okajima, K., Oike, Y., Ito, Y., Fukudome, K., Isobe, H., Suda, T., 2004. Activated
760 protein C induces endothelial cell proliferation by mitogen-activated protein kinase activation in
761 vitro and angiogenesis in vivo. Circ Res 95, 34-41.

762 Wang, L., Chen, G., Xiao, G., Han, L., Wang, Q., Hu, T., 2020. Cylindrospermopsin induces
763 abnormal vascular development through impairing cytoskeleton and promoting vascular

764 endothelial cell apoptosis by the Rho/ROCK signaling pathway. Environmental Research,
765 109236.
766 Wang, Q., Liu, Y., Guo, J., Lin, S., Wang, Y., Yin, T., Gregersen, H., Hu, T., Wang, G., 2019.
767 Microcystin-LR induces angiodysplasia and vascular dysfunction through promoting cell
768 apoptosis by the mitochondrial signaling pathway. Chemosphere 218, 438-448.
769 Wiedemann, C., Amann, B., Degroote, R.L., Witte, T., Deeg, C.A., 2020. Aberrant Migratory
770 Behavior of Immune Cells in Recurrent Autoimmune Uveitis in Horses. Front Cell Dev Biol 8,
771 101.
772 Xing, X., Kang, J., Qiu, J., Zhong, X., Shi, X., Zhou, B., Wei, Y., 2018. Waterborne exposure to
773 low concentrations of BDE-47 impedes early vascular development in zebrafish
774 embryos/larvae. Aquat Toxicol 203, 19-27.
775 Xu, X., Hou, X., Han, M., Qiu, S., Li, Y., 2019. Simultaneous determination of multiclass plant
776 growth regulators in fruits using the quick, easy, cheap, effective, rugged, and safe method
777 and ultra-high performance liquid chromatography-tandem mass spectrometry. J Sep Sci.
778 Xu, X., Liu, S., Aodengqimuge, Wang, H., Hu, M., Xing, C., Song, L., 2017. Arsenite Induces
779 Vascular Endothelial Cell Dysfunction by Activating IRE1alpha/XBP1s/HIF1alpha-Dependent
780 ANGII Signaling. Toxicol Sci 160, 315-328.
781 Yuan, X., Han, L., Fu, P., Zeng, H., Lv, C., Chang, W., Runyon, R.S., Ishii, M., Han, L., Liu, K.,
782 Fan, T., Zhang, W., Liu, R., 2018. Cinnamaldehyde accelerates wound healing by promoting
783 angiogenesis via up-regulation of PI3K and MAPK signaling pathways. Laboratory
784 Investigation 98, 783-798.
785 Zeraik, A.E., Galkin, V.E., Rinaldi, G., Garratt, R.C., Smout, M.J., Loukas, A., Mann, V.H.,

786 Araujo, A.P., DeMarco, R., Brindley, P.J., 2014. Reversible paralysis of Schistosoma mansoni
787 by forchlorfenuron, a phenylurea cytokinin that affects septins. International Journal for
788 Parasitology 44, 523-531.
789 Zhang, H.Z., Li, C.Y., Wu, J.Q., Wang, R.X., Wei, P., Liu, M.H., He, M.F., 2018.
790 Anti-angiogenic activity of para-coumaric acid methyl ester on HUVECs in vitro and zebrafish
791 in vivo. Phytomedicine 48, 10-20.
792 Zhang, L., Wei, J., Ren, L., Zhang, J., Yang, M., Jing, L., Wang, J., Sun, Z., Zhou, X., 2017.
793 Endosulfan inducing apoptosis and necroptosis through activation RIPK signaling pathway in
794 human umbilical vascular endothelial cells. Environ Sci Pollut Res Int 24, 215-225.
795 Zhang, M., Zhu, R., Zhang, L., 2019. Triclosan stimulates human vascular endothelial cell
796 injury via repression of the PI3K/Akt/mTOR axis. Chemosphere 241, 125077.
797 Zhong, X., Kang, J., Qiu, J., Yang, W., Wu, J., Ji, D., Yu, Y., Ke, W., Shi, X., Wei, Y., 2019a.
798 Developmental exposure to BDE-99 hinders cerebrovascular growth and disturbs vascular
799 barrier formation in zebrafish larvae. Aquat Toxicol 214, 105224.
800 Zhong, X., Qiu, J., Kang, J., Xing, X., Shi, X., Wei, Y., 2019b. Exposure to
801 tris(1,3-dichloro-2-propyl) phosphate (TDCPP) induces vascular toxicity through Nrf2-VEGF
802 pathway in zebrafish and human umbilical vein endothelial cells. Environ Pollut 247, 293-301.
803

Highlights：

CPPU induced abnormal vascular development in zebrafish embryo.

CPPU inhibited FAK/MEK/ERK/JNK phosphorylation in HUVECs.

Toxicity of CPPU correlated to impairments of cytoskeleton and migratory signaling.

Declaration of interests

☒ The authors declare that they have no known competing financial interests or personal relationships that could have appeared to influence the work reported in this paper.

☐The authors declare the following financial interests/personal relationships which may be considered as potential competing interests:

None